Geochemistry and petrography of amphibolites from the Spuhler Peak Metamorphic Suite near the Branham Lakes area, Tobacco Root Mountains, southwestern Montana

M. Jason Cox
Department of Geology, Washington and Lee University, Lexington, VA 24450
Faculty sponsor: Samuel J. Kozak, Washington and Lee University

INTRODUCTION

Located in the Sheridan district of the west-central Tobacco Root Mountains in southwestern Montana, the Spuhler Peak Metamorphic Suite (SPMS) of Gillmeister (1972) represents an assemblage of Archean-age, cordierite-amphibolite facies rocks (Burger, 1969) that has been interpreted to structurally overly the Indian Creek Metamorphic Suite (ICMS) and rest beneath the Pony-Middle Mountain Metamorphic Suite (PMMMS). The lithologic assemblage of the SPMS consists of lensoid amphibolite beds, more equant bodies of "wispy" amphibolite, pods of ultramafic rocks, hornblende-plagioclase gneisses, garnet-gedrite gneisses, quartzites, and sillimanite schists. This wide range of lithologies complicates interpretations regarding the relationships between protoliths. The schists, gneisses, and quartzites, interpreted as metasedimentary rocks, are concordantly layered with amphibolites and ultramafic rocks, interpreted metaigneous rocks. Previous workers in this area have failed to demonstrate that the protoliths of these amphibolites are igneous and not sedimentary. Field observations of these amphibolites provide little evidence concerning their protoliths. While some outcrops possess a planar foliation and a mineral lineation, these characteristics do not necessarily indicate a sedimentary protolith for metamorphic rocks (Leake, 1969). In this study, an attempt is made to identify the amphibolites' protolith and determine their tectonic setting by an evaluation of their geochemistry.

METHODS

More than two-hundred samples of amphibolites were collected from a variety of locations mostly within the area from Noble Peak and Mustard Pass in the northwest to Lower Branham Lake in the southeast. Thirty-one of these were selected for chemical analyses of major and trace elements by XRF at XRAL Laboratories or at Franklin and Marshall College, and INAA analysis for selected rare earth elements at the University of Virginia. Twenty-six samples, most of which were chemically analyzed, were thin-sectioned and their petrography studied.

GEOCHEMISTRY

The problem of distinguishing between ortho- and para-amphibolites has long concerned many geologists, but few new methods have been developed in the last 25 years to accomplish it. Leake (1969) and van de Camp (1969) attempt to distinguish between an igneous or sedimentary protolith for amphibolites by means of variation diagrams using Niggli values (Niggli, 1954). On a plot of al-alk vs. c (Fig.1), the SPMS amphibolites plot in an area where a trend from anorthosite toward basalts crosses an area of clay and dolomite mixtures and fails to support unequivocally either a sedimentary or igneous origin for the protolith. A plot of c versus mg (Fig.2) indicates that the SPMS amphibolites follow the same trend as the Karroo dolerites (Evans and Leake, 1960). Plots of mg vs. Cr (Fig.3) and mg vs. Ni (Fig.4) show the SPMS amphibolites having trends with positive slopes such as those found in igneous but not shale-carbonate rocks. In addition, the SPMS samples follow the trend from early basic to late basic igneous rocks when plotted on a 100*mg+c+(al-alk) diagram (Fig.5).

Since Niggli plots of SPMS amphibolites suggest an igneous protolith, plots of SiO2 vs. (Na2O+K2O) (Fig.6) and Alkalies-FeO-MgO (Fig.7) are used to characterize the basalt in present-day parameters. All of the SPMS amphibolites plot as subalkaline on the SiO2 vs. alkalies plot, and all plot in the field of tholeiitic basalts on the AFM diagram.

A number of workers have used variation diagrams to correlate various compositional parameters with modern tectonic environments (Pearce and Cann, 1973, Mullen, 1983, and Meschede, 1986). Pearce and Cann (1973) utilized discriminant analysis to assign basalts to modern tectonic environments, identifying ocean floor basalts (OFB) with diverging plate margins, volcanic arc basalts (VAB) with converging plate margins, ocean island basalts (OIB) with within-plate oceanic crust, and continental basalts (CB) with within plate-continental crust. Plots of SPMS amphibolites on some of these tectonic discrimination diagrams do not correlate their protoliths with any one tectonic environment. A plot of Zr-(Ti/100)-(Y*3) (Fig.8) (Pearce and

Cann, 1973) shows a distribution in the fields of OFB (19 samples), calc-alkali basalts (CAB) (5), and within-plate basalts (OIB or CB) (4). On a plot of Zr-Ti/100-Sr/2 (Fig.9) (Pearce and Cann, 1973), the SPMS amphibolites plot in the fields of IAB (5), CAB (7), and OFB (13). A plot of Zr. vs. Ti (Fig.10) (Pearce and Cann, 1973) shows SPMS amphibolites lying in the fields of island-arc basalts (6), ocean-floor basalts(12), calc-alkali basalts (4), and in a field containing OFB, IAB, and CAB (6). The SPMS amphibolites appear to be more constrained in a plot of MgO-FeO(total)-Al2O3 (Fig.11) (Pearce et al., 1977). In it they appear largely confined to the OIB field (20), with a few (6) plotting in the continental basalt field and (3) in the ocean ridge field. A Nb-Zr-Y plot (Fig.12) (Meschede, 1986) indicates that the SPMS samples are distributed between four tectonic environments: normal-MORB/volcanic-arc basalts (15), plume-type-MORB/VAB (7), within-plate tholeiites (1), and OFB/LKT/CAB (4). Volcanic-arc basalts and MORB's are not clearly distinguishable on this diagram. On a plot of MnO-TiO2-P2O5 (Fig.13) (Mullen, 1983), the SPMS amphibolites plot in the fields of island-arc tholeiites (16), CAB (13), and MORB (1). Most of the tectonic discrimination diagrams, especially those of Pearce and Cann (1973), suggest that the SPMS amphibolites have an ocean-floor basalt as a protolith. A summary of the distributions of SPMS amphibolites to tectonic environments is shown in Table 1.

PETROGRAPHY

While most thin sections demonstrate characteristics common to amphibolites, variations in mineral composition and textures do occur. The samples vary in color, mineral contents, and grain size. Few thin sections show any preferred orientation. Most of the samples consist of the assemblage hornblende-plagioclase-quartz, with varying amounts (if any) of garnet, biotite, chlorite, cummingtonite, ground-up material termed "grunge", and opaques such as magnetite and pyrite. Samples collected adjacent to the contact with the late Mesozoic Tobacco Root Batholith contain more biotite probably due to alteration by contact with this hot body. Muscovite and biotite are more abundant in samples from the Leggat cirque area near the contact with the ICMS than in most of the other SPMS amphibolites. Garnet increases in abundance in the disturbed zone (up to 45%) and as one approaches the contact with the ICMS, suggesting higher pressure. The anorthite content of the plagioclases in different samples ranges from Ab70-An30 to Ab35-An65, with an average of Ab60-An40. The varying modal amounts of hornblende and plagioclase, sometimes with significant amounts of quartz, suggests that some samples are hornblende-plagioclase-quartz gneisses.

CONCLUSIONS

From the plots originally devised by Evans and Leake (1960), the SPMS amphibolites are interpreted to be of igneous and not sedimentary origin. Other plots (Figs. 6 & 7) characterize the igneous protolith of the SPMS amphibolites as subalkaline and tholeiitic basalts. While plots on tectonic discrimination diagrams are somewhat dispersed possibly due to composition changes caused by the relatively high grade of metamorphism, most samples plot as ocean-floor basalts (OFB). However, one should remain cautious in making interpretations about tectonic environments as a lack of detailed information regarding plate-tectonics in the Archean still exists.

REFERENCES CITED

Burger, H. R., 1969, Structural evolution of the southwestern Tobacco Root Mountains, Montana: Geological Society of American Bulletin, v. 80, p. 1329-1342.

Evans, B. W., and Leake, B. E., 1960, The Composition and Origin of the Striped Amphibolites of Connemara, Ireland: Journal of Petrology, v. 1, p. 337-363.

Gillmeister, N. M., 1972, Cherry Creek Group-Pony Group relationship in the central Tobacco Root Mountains, Madison County, Montana: Northwest Geology, v. 1, p. 21-24.

Leake, B. E., 1969, The Discrimination of Ortho and Para Charnokitic Rocks, Anorthosites and Amphibolites: The Indian Mineralogist, v. 10, p. 89-104.

Meschede, M., 1986, A Method of Discriminating Between Different Types of Mid-Ocean Ridge Basalts and Continental Tholeiites with the Nb-Zr-Y Diagram: Chemical Geology, v. 56, p. 207-218.

Mullen, E. D., 1983, MnO/TiO2/P2O5: a minor element discrimination for basaltic rocks of oceanic environments and its implications for petrogenesis: Earth and Planetary Science Letters, v. 62, p. 53-62.

Niggli, P., 1954, Rocks and Mineral Deposits: San Francisco, Freeman, 559 p. [book]

Pearce, J. A.., and Cann, J. R., 1973, Tectonic Setting of Basic Volcanic Rocks Determined Using Trace Element Analyses: Earth and Planetary Science Letters, v. 19, p. 290-300.

Pearce, T. H., Gorman, B. E., and Birkett, T. C., 1977, The relationship between major element chemistry and tectonic environment of basic and intermediate volcanic rock: Earth and Planetary Science Letters, v. 36, p. 121-132.

van de Camp, P. C., 1969, Origin of Amphibolites in the Beartooth Mountains, Wyoming and Montana: New Data and Interpretation: Geological Society of America Bulletin, v. 80, p. 1127-1136.

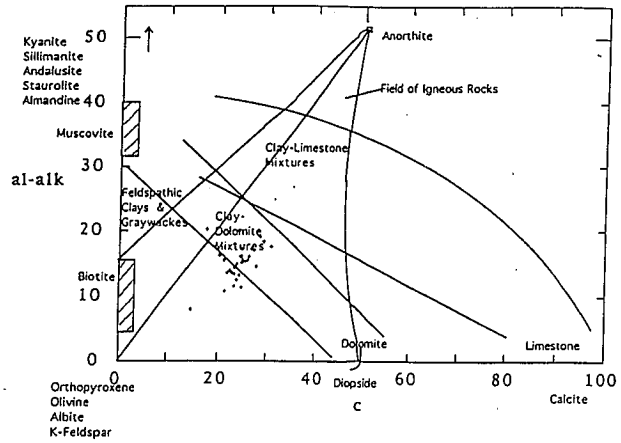

Figure 1: Leake (1969): Plot of Niggli al-alk against c for igneous and sedimentary rocks. The SPMS amphibolites plot in the fields for both types of rocks and do not follow a distinctive igneous or sedimentary trend.

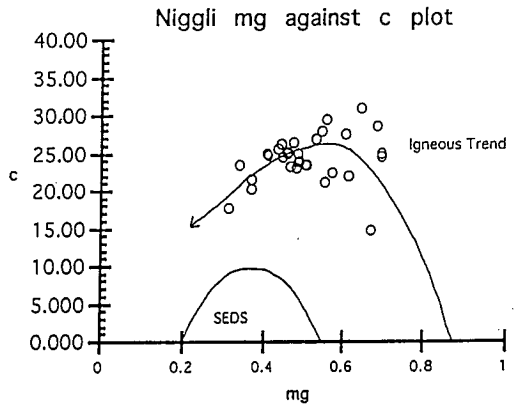

Figure 2: The SPMS amphibolites show an igneous trend similar to the Karroo dolerites (Evans and Leake, 1960) when plotted on a Niggli mg vs. c diagram.

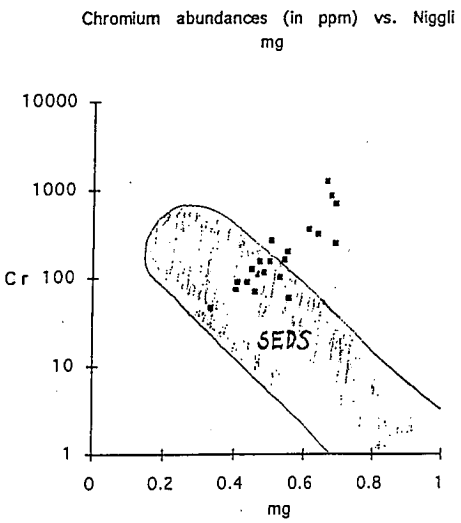

Figure 3: When plotted on a Cr (in ppm) against mg diagram, the SPMS amphibolites demonstrate a positive slope indicative of igneous rocks but not shale-carbonate rocks.

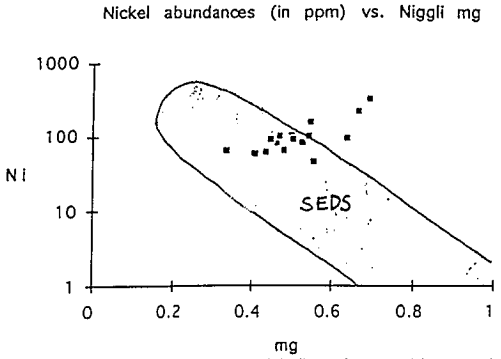

Figure 4: The SPMS amphibolites show positive correlations indicative of basic igneous rocks but not shale-carbonate rocks when plotted on a Ni vs. Niggli mg diagram.

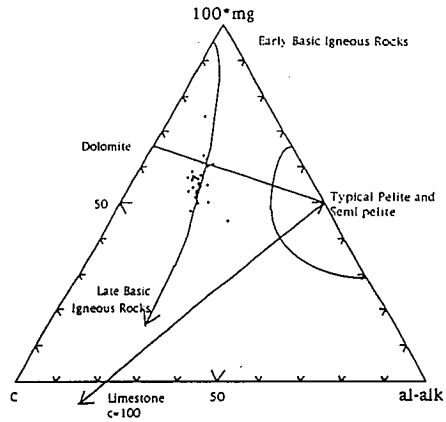

Figure 5: The SPMS amphibolites follow the trend from early basic to late basic igneous rocks when plotted on a 100*mg+c+(al-alk) diagram.

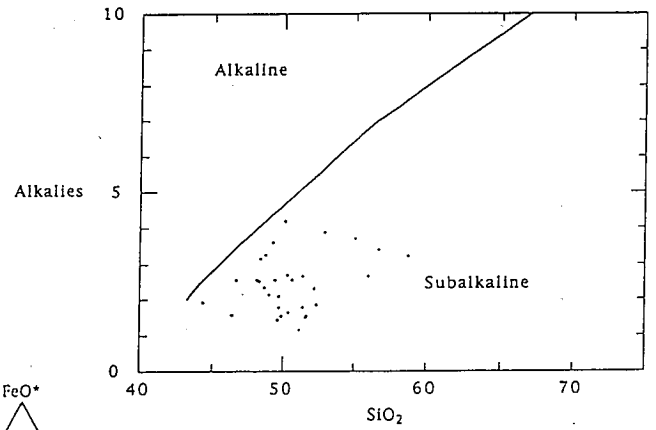

Figure 6: All of the SPMS amphibolites plot as subalkaline on the plot of SiO2 vs. (Na2O+K2O) or Alkalies

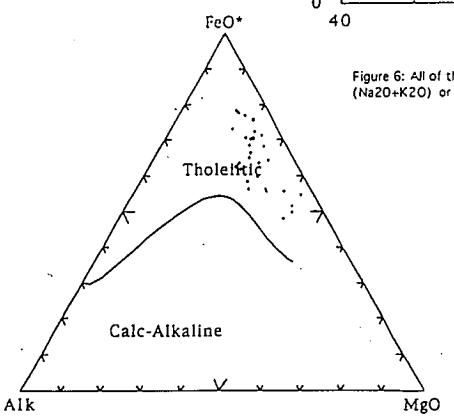

Figure 7: All samples of the SPMS amphibolites plot in the field of Tholeiitic basalts on the AFM diagram.

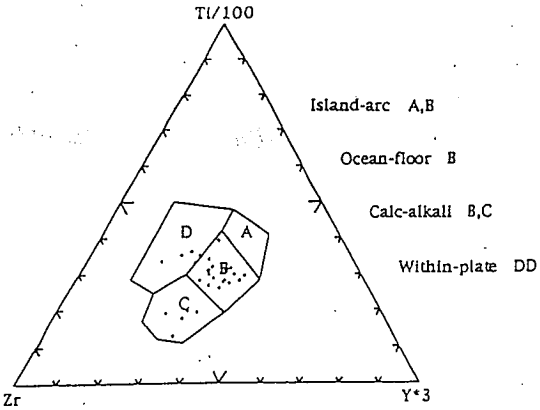

Figure 8: The Pearce and Cann (1973) Zr-Ti/100-Y*3 discriminant diagram. The SPMS amphibolites plot mostly as ocean-floor basalts (24). Note the overlap of OFB's and IAB's in the B field.

Tectonic Discriminant Diagram Summary						
	Diagram					
Environment	Mullen	Meschede	MgO-FeO-AlO	Zr-Ti Diag.	Zr-Ti-Sr	Zr-Ti-Y
OceanFloorBasalts		4	3	18	13	24
IslandArcBasalts	14	26	20	12	5	19
CalcAlkaliBasalts	13	4		4	7	5
ContinentalBasalts			6			
WithinPlateBasalts		1				4
MOR Basalts	1	26	3			

Table 1: A summary of the distribution of the SPMS amphibolites plotted on 6 different tectonic discriminant diagrams. Some overlap occurs on the diagrams as distinguishing between tectonic environments can prove impossible using certain major and trace elements. The majority of SPMS amphibolites plot as ocean-floor basalts on Pearce and Cann (1973) diagrams. Meschede does not separate the field for island-arc basalts and MORB's on the Nb-Zr-Y plot. The SPMS amphibolites plot mainly as island-arc basalts on the MgO-FeO-AlO diagram (Pearce et al., 1977).

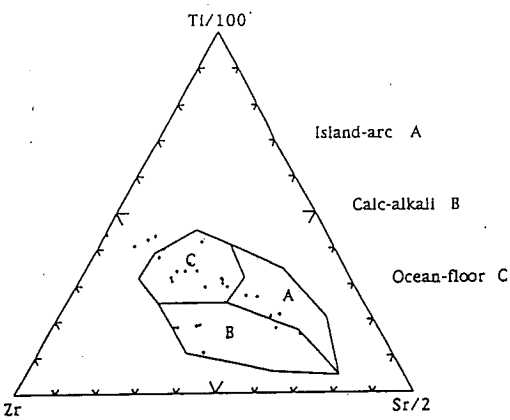

Figure 9: The SPMS amphibolites plot mostly as ocean-floor basalts (13), calc-alkali basalts (7), and island-arc basalts (5) on the Zr-Ti/100-Sr/2 diagram (Pearce and Cann, 1973).

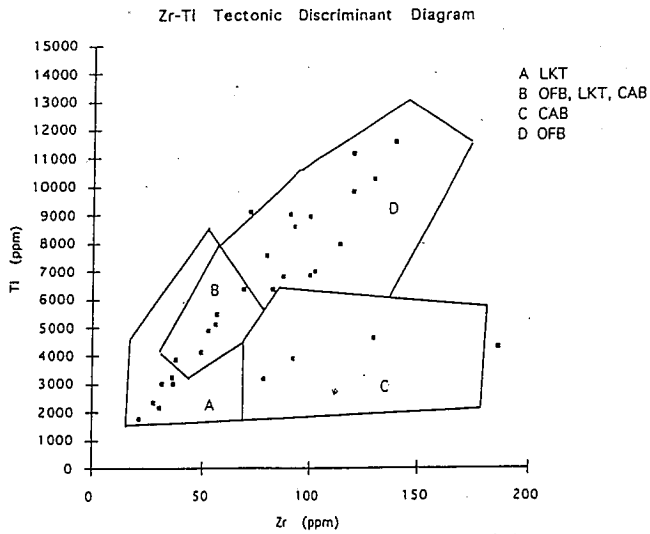

Figure 10: The SPMS amphibolites plot mostly as ocean-floor basalts (18) and low potassium tholeiites (12), associated with island-arc basalts, on the Ti-Zr discrimination diagram of Pearce and Cann (1973).

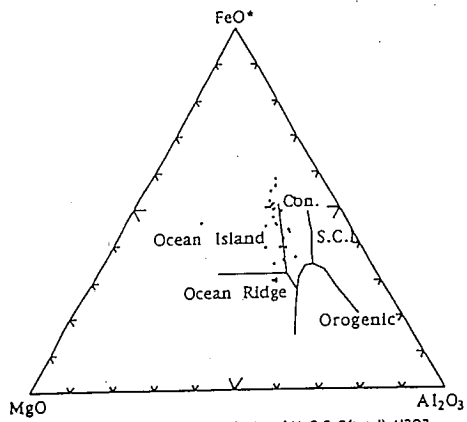

Figure 11: The Pearce et al. (1977) plot of MgO-FeO(total)-Al2O3. The SPMS amphibolites plot in the fields of Ocean-Island Basalts (20). Continental Basalts (6), and Oceanic Ridge/Floor Basalts (3). S.C.I= Spreading Center Island Basalts.

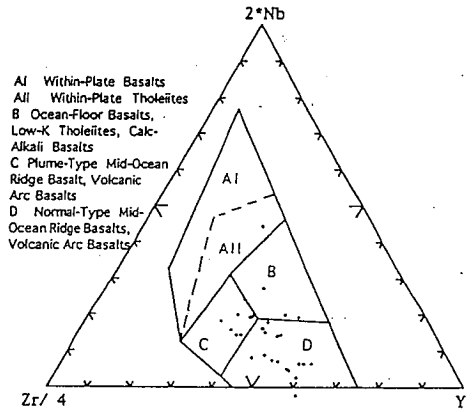

Figure 12: The SPMS amphibolites plotted on the Meschede (1986) Nb-Zr-Y diagram Meschede does not reasonably differentiate the fields of MORB's and VAB's.

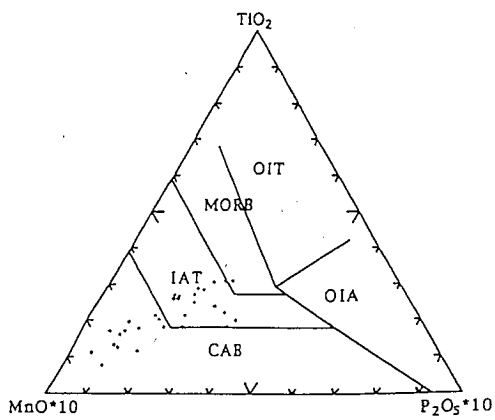

Figure 13: The Mullen (1983) MnO*10-TiO2-P2O5*10 diagram. OIT=Ocean Island Tholeiites, MORB=Mid Ocean Ridge Basalts, IAT=Island Arc Tholeiites, and CAB=Calc-Alkali Basalts. The SPMS amphibolites plot mainly as Island Arc Tholeiites (14) and Calc-Alkali Basalts (13).